Reduction of High-Affinity β_2-Adrenergic Receptor Binding by Hyperforin and Hyperoside on Rat C6 Glioblastoma Cells Measured by Fluorescence Correlation Spectroscopy

Lars Prenner,[‡] Anne Sieben,[‡] Karin Zeller,[§] Dieter Weiser,[§] and Hanns Häberlein*[,‡]

Institute of Physiological Chemistry, Rheinische Friedrich-Wilhelms University of Bonn, Germany, and Steigerwald Arzneimittelwerk GmbH, Darmstadt, Germany

Received December 15, 2006; Revised Manuscript Received March 7, 2007

ABSTRACT: β-Adrenergic receptors (β-AR) are potential targets for antidepressants. Desensitization and downregulation of β-AR are discussed as possible modes of action for antidepressants. We have investigated the effects of hyperforin and hyperoside, compounds with potentially antidepressant activity from St. John's Wort, on the binding behavior and dynamics of β_2-AR in living rat C6 glioblastoma cells, compared to desipramine (desmethylimipramine; DMI) by means of fluorescence correlation spectroscopy (FCS) and fluorescence microscopy. FCS-binding studies with the fluorescently labeled ligand Alexa532-noradrenaline (Alexa532-NA) binding to β_2-AR of C6 cells showed a significant reduction in total β_2-AR binding after preincubation with hyperforin and hyperoside for 3 days, respectively, which was also found for DMI. This was mainly observed in high-affinity receptor−ligand complexes with hindered lateral mobility (D_2 = 1.1 (±0.4) μm^2/s) in the biomembrane. However, internalization of β_2-AR was found neither in *z*-scans of these C6 cells nor in HEK 293 cells stably transfected with GFP-tagged β_2-adrenergic receptors (β_2AR-GFP) after incubation up to 6 days with either DMI, hyperforin, or hyperoside. Thus, under these conditions reduction of β_2-AR binding was not mediated by receptor internalization. Additionally, preincubation of C6 cells with DMI, hyperforin, and hyperoside led to a loss of second messenger cAMP after β_2-adrenergic stimulating conditions with terbutaline. Our current results indicate that hyperforin and hyperoside from St. John's Wort, as well as DMI, reduce β_2-adrenergic sensitivity in C6 cells, emphazising the potential usefulness of St. John's Wort dry extracts in clinical treatment of depressive symptoms.

Depressive disorders are some of the most common mental diseases, affecting approximately 20% of the population (*1*). Therapy is centered on the use of tricyclic antidepressants (TCA), selective serotonin-reuptake inhibitors (SSRI), and serotonin-noradrenaline-reuptake inhibitors (SNRI) together with preparations from St. John's Wort (*Hypericum perforatum L.*) for the treatment of mild to moderate cases (*2*−*4*). The pharmacological mode of action of both synthetic antidepressants and St. John's Wort preparations relies on noradrenaline (NA) and serotonin (5-HT) neurotransmitter metabolism. Most antidepressants interfere with synaptic communication by elevating neurotransmitter concentrations in the synaptic cleft following inhibition of reuptake. This results in a delayed adaptive alteration in neurotransmitter receptor density in certain brain areas (*2*). For β-adrenergic receptors (β-AR[1]) down-regulation is observed which can be correlated temporally with clinical antidepressant effects (*5*, *6*). Hyperforin is seen as one of the most important single active compounds responsible for the pharmacological activity of St. John's Wort dry extracts. Among others it inhibits the synaptic reuptake of 5-HT and NA (*7*, *8*). Flavonoids are also of therapeutic relevance. Hyperoside and its main metabolite miquelianine, e.g., showed antidepressant effects in the Porsolt forced-swimming test (FST) in rats (*9*). Hyperoside and other glycosylated quercetin-flavonoids influenced the hypothalamic-pituitary-adrenal-axis (HPA-axis) in animals (*10*).

Using desipramine (desmethylimipramine; DMI) as a control, we investigated the influence of hyperforin and hyperoside from St. John's Wort on β_2-AR of rat C6 glioblastoma cells, without any previous activation from presynaptic neurons. This model has already been successfully applied to studies on signal transduction and down-regulation of total β-AR. Therein, DMI influenced the interaction of G_s-proteins with effector proteins like adenylyl cyclase (AC) (*11*), leading to a densensitization of β-AR (*12*). Postsynaptic down-regulation of β-AR in C6 cells after DMI treatment has also been reported (*13*, *14*). Changes in β-AR dynamics are therefore to be expected in this model, similar to those reported previously for β_2-AR on A549 cells and hippocampal neurons under low stimulating conditions (*15*). A correlation between lateral receptor mobility and receptor

* Corresponding author. Prof. Dr. Hanns Häberlein, Institute of Physiological Chemistry, Nussallee 11, D-53115 Bonn, Germany. Tel: +49 228 736555. Fax: +49 228 732416. E-mail: haeberlein@institute.physiochem.uni-bonn.de.

‡ Rheinische Friedrich-Wilhelms University of Bonn.

§ Steigerwald Arzneimittelwerk GmbH.

[1] Abbreviations: β2-AR, β2-adrenergic receptor; FCS, fluorescence correlation spectroscopy; Alexa532-NA, Alexa Fluor 532-arterenol; DMI, desipramine.

10.1021/bi6025819 CCC: $37.00
Published on Web 04/07/2007

state has also been demonstrated for the $GABA_A$-receptor (*16*). The effect of hyperforin, hyperoside, and DMI on the lateral mobility of β_2-AR after binding of a fluorescently labeled noradrenaline derivative (Alexa532-NA) was investigated in C6 cells using fluorescence correlation spectroscopy (FCS). FCS is a powerful method allowing measurements of particle dynamics on subcellular compartments within living cells under real time conditions (*17*, *18*). FCS is therefore well suited for the observation of receptor−ligand interactions, using receptor fusion proteins or fluorescently labeled ligands (*19*). Due to its noninvasive qualities, FCS allows insights into the physiological regulatory mechanisms for membrane receptors at the single molecular level (*20*, *21*).

Furthermore, effects of DMI, hyperforin, and hyperoside on the distribution of β_2-AR-GFP fusion proteins in stably transfected HEK 293 cells have been investigated.

EXPERIMENTAL PROCEDURES

Materials. Desipramine-HCl was purchased from ICN Biomedicals. Hyperforin was obtained from HWI-Analytics. Hyperoside was obtained from Roth Chemicals. All reagents for cell culture were from Gibco BRL. Isoprenaline-sulfate and terbutaline-hemisulfate were purchased from Sigma. All other reagents were obtained from Merck or Sigma and of the highest purity available.

Fluorescence Correlation Spectroscopy. FCS measurements were performed with a ConfoCor instrument (Zeiss) equipped with an argon laser LGK 7812 ML 2 (Lasos) and a water immersion objective C-Apochromat, 63×, NA 1.2 (Zeiss). Size of the illuminated volume element was 0.19 fL. For excitation the 514 nm line was used. Power density in the focal plane, measured before the objective, was $p_{514\,nm} = 14.2-109$ kW/cm^2. The emitted fluorescence was separated from the excitation light with a dichroic filter and a bandpass filter; wavelength splitting at 514 nm: FT 540, EF 530−600 (Zeiss). The fluorescence intensity fluctuations were detected by an avalanche single photon counting module SPCM-AQ series (EG & G Optoelectonics). The signal was correlated online to data acquisition with a digital hardware correlator ALV-5000 (ALV). Prior to experiments, the volume element of observation was calibrated. For this purpose, autocorrelation functions for the dye diffusion of 10 nM tetramethylrhodamine (TMR) (Invitrogen) in binding buffer were recorded. The radii $\omega_0 = 0.19$ μm and $z_0 = 1.08$ μm were calculated (according to eqs 1 and 3) from the determined diffusion time constant for TMR and a diffusion coefficient of 280 μm^2/s (*22*). Laser cell scans were performed by moving the focus in the *z*-direction through the cell to characterize the initial autofluorescence and the fluorescence intensity after ligand incubation in C6 cells. Cells which showed a typical 2-peak profile, with the cytosol representing an area of low fluorescence, were chosen for FCS measurements if the magnitude of fluorescence did not exceed certain boundaries. For the ligand binding studies, taking the position of the half-maximal autofluorescence of the upper membrane, the focus took in fast diffusing free ligand and slow diffusing receptor−ligand complexes.

Single Particle Tracking. Trajectories of single receptor−ligand complexes were measured with a TE2000 mikroscope (Nikon) equipped with a CFl objective Plan Apo VC 60x WI, a GLK 3250 T01 continuous-wave diode-pumped solid-state laser (Lasos), and a iXon DV 860 BI camera (Andor Technologies) used in combination with a 4-fold magnifier. Laser power was 2 mW. For excitation a 532 nm line with an intensity of 1.87 kW/cm^2 was used. Exposure time was 10 ms with a kinetic cycling time of 10.22 ms. Alexa532-NA concentration was 1 nM.

Fluorescence Microscopy. Fluorescence microscopy was performed with a fluorescent microscope Axiovert 100M, oil immersion objective Plan Neofluar 100×, NA 1.3; camera, Axiocam HRm; lamp, HBO 50; software, Axiovision 3.1 (Zeiss).

Pictures shown are representative of 3 independently performed experiments.

Data Analysis. Data from FCS calibration measurements with free dye in solution and from fluorescently labeled ligand in solution, respectively, were calculated with the three-dimensional autocorrelation function (eq 1) according to a three-dimensional Gaussian volume:

$$G(\tau) = 1 + \frac{\sum_{j=1}^{n} Q_j^2 N_j}{[\sum_{j=1}^{n} Q_j N_j]^2} \frac{1}{1 + \tau/\tau_{D_j}} \sqrt{\frac{1}{1 + (w_0/z_0)^2 \tau/\tau_{D_j}}} \quad (1)$$

and

$$Q_j = \sigma_j \eta_j g_j \quad (2)$$

where ω_0 is the radius of the observation volume in the focal plane, z_0 is the radius of the observation volume in the *z*-direction, D_j is the translational diffusion coefficient of the species *j*, N_j is the average number of molecules of the species *j* in the volume element, τ_{D_j} is the mean diffusion time constant of the species *j* through the volume element, Q_j is the quantum yield factor, σ_j is the absorption cross section, η_j is the fluorescence quantum yield, and g_j is the fluorescence detection efficiency of the species *j*.

The diffusion coefficient D_j and the diffusion time constant τ_{D_j} in the focus correlate as shown in eq 3:

$$\tau_{D_j} = \frac{\omega_0^2}{4D_j} \quad (3)$$

A simplified autocorrelation function $G(\tau)$ (eq 4), which accounts for a two-dimensional diffusion of receptor−ligand complexes in the cell membrane and the same count rate per molecule for all fluorescent components *j* (i.e., all Q_j are the same), was used for data analysis of the ligand binding studies:

$$G(\tau) = 1 + \frac{1}{N} \sum_{j=1}^{n} \frac{y_j}{1 + \tau/\tau_{D_j}} \quad (4)$$

where y_j is the fraction of the species *j* to the autocorrelation amplitude, *N* is the total number of molecules in the detection volume element, and τ_{D_j} is the diffusion time constant of the species j.

For parametrization and fitting of the autocorrelation function $G(\tau)$, a nonlinear least-squares minimization was performed according to the Marquardt algorithm (*23*).

Alexa532-NA. Synthesis, analytics, and specificity of fluorescently labeled noradrenaline (Alexa532-NA) at the β_2-AR were reported by our group previously (*15*).

C6 Cells. Rat C6 glioblastoma cells (DSMZ, No. ACC 550) were cultivated in DMEM-F12 medium + glutamine 2 mM + penicillin/streptomycin 100 U/mL + 5% fetal calf serum in 10 cm cell culture dishes (Falcon) at 37 °C and 5% CO_2 and saturated humidity. Cells were used for experiments between passages 10 and 30.

Stable Transfection of HEK293 Cells. Human embryonic kidney cells (HEK293) (DSMZ, No. ACC 305) were stably transfected with DNA encoding the β_2-AR as a GFP fusion protein (β_2AR-GFP) (*24*). The β_2AR-GFP plasmid (2 μg) was mixed with ExGene-reagent (Fermentas) (6.6 μL) following the manufacturer's instructions and added to the cells in 3.5 cm cell culture dishes (Sarstedt) in a density of ~25 000 cells for 3 h. Transfected cells were selected by adding G418-sulfate (500 μg/mL; PAA Laboratories GmbH) 72 h after transfection to the culture medium. Transfected cells were identified after 2 weeks by fluorescence microscopy. Cells were further seeded into 96-well cell culture dishes (Sarstedt) to establish the clonal HEK293β_2AR-GFP cell line. Cells were cultivated in DMEM-F12 medium + glutamine 2 mM + penicillin/streptomycin 100 U/mL + 5% fetal calf serum in 10 cm cell culture dishes (Falcon).

Cells were used for experiments between passages 10 and 30.

Live Cell Experiments. For live cell FCS, single particle tracking, and fluorescence microscopy experiments, cells were plated onto heat-sterilized glass coverslips for microscopy (#1, Ø 18 mm, Menzel-Gläser) in a density of 2.5−5 × 10^4 cells/cm^2 in 12× multiwell chambers (Nunc) and cultivated for 2 to 4 days at 37 °C and 5% CO_2 in an incubator. Cells were then grown to 70−80% confluency before using in experiments. Preincubation of the cells was done for 3 to 6 days by addition of 1 μM desipramine-HCl (stock solution 1 mM in H_2O (aqua ad injectabilia)), hyperforin (stock solution 1 mM in methanol), and hyperoside (stock solution 1 mM in 50% methanol (v/v)) to the culture medium. Control cells and any other cells were added a maximum of 0.1% methanol as vehicle. Prior to measurements cells were washed three times with Lockes' solution pH 7.4 (NaCl 9.00 g, KCl 0.42 g, $CaCl_2$ dihydrate 0.34 g, $MgCl_2$ hexahydrate 0.20 g, $NaHCO_3$ 0.30 g, HEPES 1.26 g, D(+)-glucose monohydrate 3.96 g, aqua bidest. ad 1000.0 mL) at 37 °C. The coverslips were mounted on a coverslip carrier above the microscope objective with an incubation volume of 400 μL. For the ligand binding studies, C6 cells were incubated for 15 min with 10 nM Alexa532-NA in Lockes' solution. All measurements were performed at 20 °C, and cells were used for at best 60 min. Data of all experiments were analyzed with Origin 7.5 software (OriginLab Corp.).

cAMP-Assay. C6 cells were seeded in a density of 6000 cells/well in 96-well cell culture dishes (Sarstedt) and pretreated, where indicated, with test substances for 3 days in 100 μL of DMEM-F12 medium + glutamine 2 mM + penicillin/streptomycin 100 U/mL + 5% fetal calf serum at 37 °C, 5% CO_2 in an incubator. The cells were serum-starved for 10 min and further incubated, where indicated, with 10 μM of the β_2-adrenergic agonist terbutaline-hemisulfate or with phosphate buffer solution (10 mM PBS pH 7.4: KH_2PO_4 0.26 g, $Na_2HPO_4 \cdot 7H_2O$ 2.17 g, NaCl 8.71 g, aqua bidest. ad 1000.0 mL) in control cells for 30 min at 37 °C. The intracellular concentration of cyclic adenosine monophosphate (cAMP) was determined with a HitHunter cAMP Assay-kit for adherent cells based on EFC (enzyme fragment complementation)-chemiluminescence-detection (DiscoveRx), following the manufacturer's instructions. The 96-well plates were measured using a fluorescence reader Tecan GENios (Tecan) using chemiluminescence mode at 1 s/well. Data processing was done with Magellan 3.0 software (Tecan).

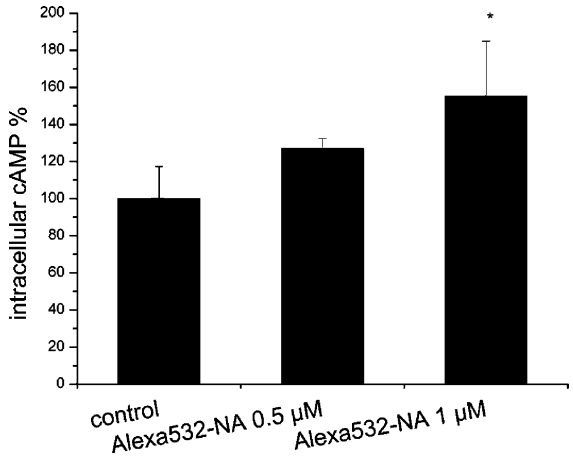

FIGURE 1: Accumulation of intracellular cAMP in C6 cells comparing control cell levels with cells incubated with 0.5 μM and 1 μM Alexa532-NA ($n = 3$) (*$p < 0.05$).

Statistical Data Evaluation. Statistical significance of results was proven with one factorial analysis of variance (ANOVA). All data points from live cell FCS experiments represent mean values (±) standard deviation (SD) of 5 measurements per cell from at least 3 different cells. Experiments were performed at least twice independently. Results with p-values <0.05 were determined statistically significant, and results with p-values <0.01 were determined statistically highly significant.

RESULTS

β_2-Adrenergic receptor (β_2-AR) binding studies on C6 cells were performed using FCS and a fluorescently labeled noradrenaline (Alexa532-NA). Alexa532-NA binds selectively to β_2-AR (*15*) and mediated a dose-dependent increase in intracellular cAMP formation. After incubation of C6 cells with 0.5 μM and 1 μM of Alexa532-NA, respectively, cAMP levels increased by 27.1 (±1.1)% and 55.2 (±10.6)% ($n = 3$) (Figure 1). C6 cells incubated with 10 nM Alexa532-NA for 15 min showed a total binding of 4.26 (±0.53) nM ($n = 72$). Under these conditions endocytotic internalization of receptor−ligand complexes was not found in laser-aided C6 cell z-scans, whereas stronger stimulation of cells with 1 μM terbutaline led to internalization of receptor−ligand complexes (Figure 2). Analysis of the binding data revealed a diffusion time constant of $\tau_{free} = 39.9$ (±2.3) μs and a diffusion coefficient of $D_{free} = 214.0$ (±11.8) $\mu m^2/s$ for freely diffusing Alexa532-NA, whereas the receptor−ligand complex showed two different lateral mobilities with $\tau_{Diff1} = 0.65$

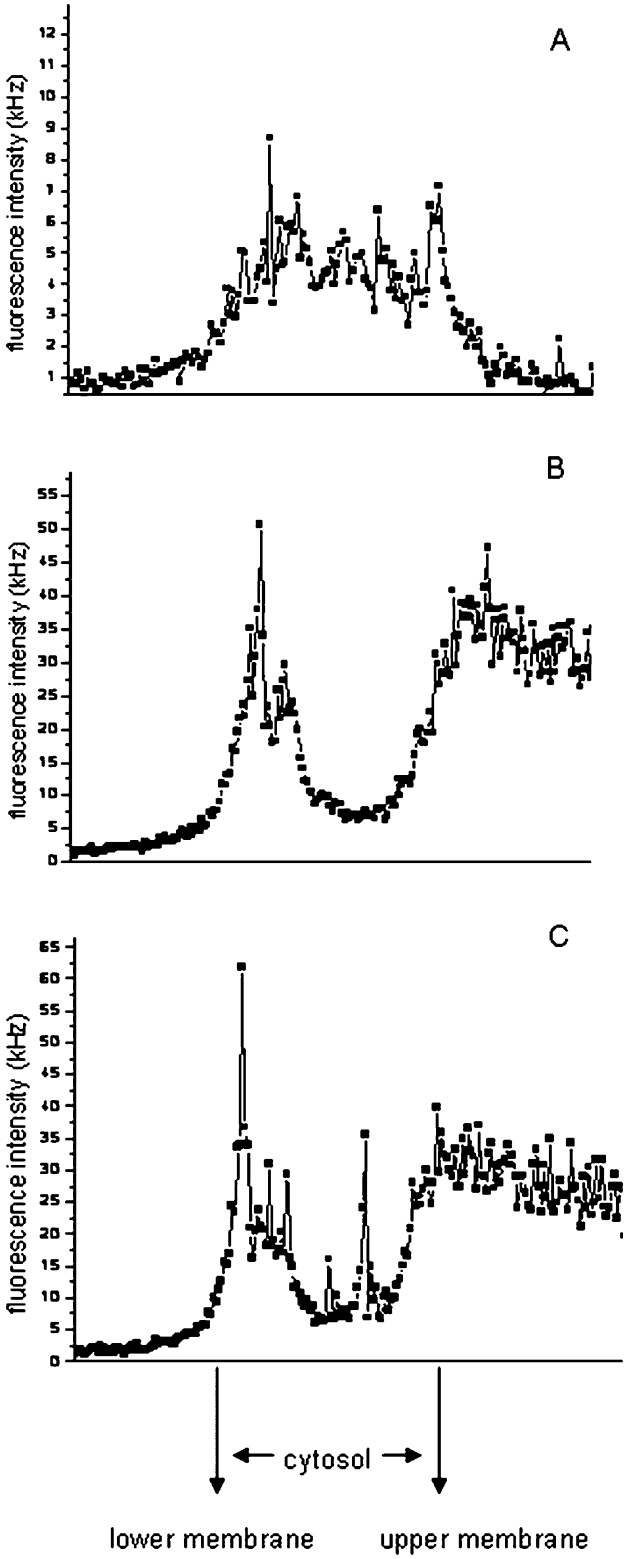

FIGURE 2: Cell *z*-scans of single C6 cells: (A) unincubated control cell; (B) cell incubated with 10 nM Alexa532-NA for 15 min; (C) cell incubated with 10 nM Alexa532-NA for 15 min and subsequent incubation with 1 μM terbutaline for 20 min; *z*-scans shown are representative of at least 3 scans performed independently.

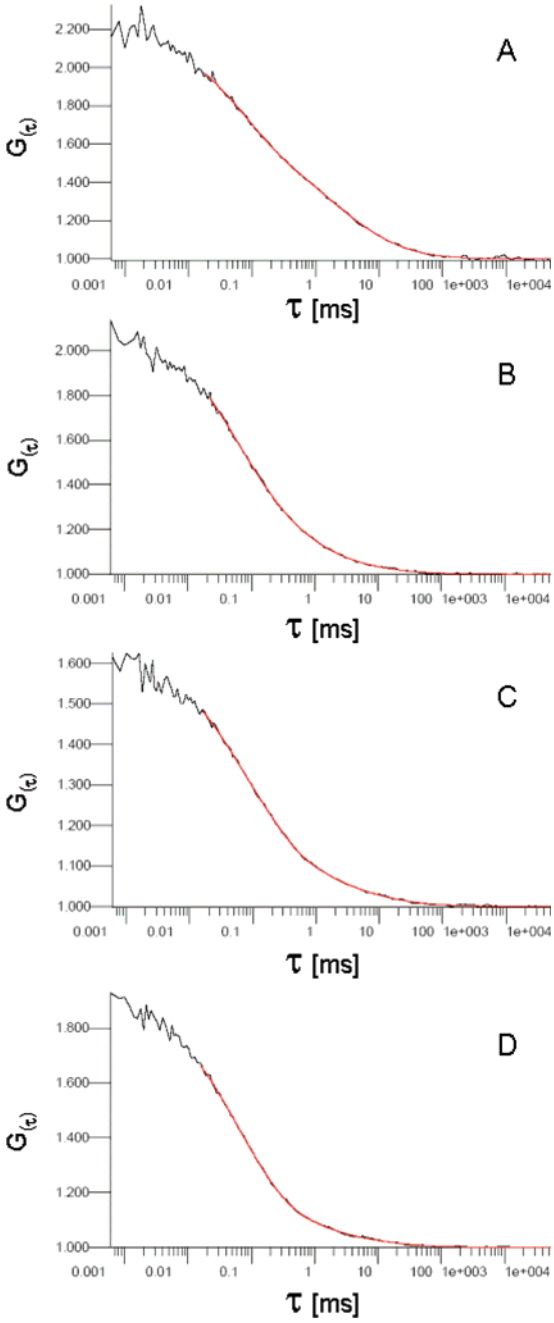

FIGURE 3: Autocorrelation curves (red, fit functions) derived from 30 s FCS measurements in the biomembrane of C6 cells incubated with 10 nM Alexa532-NA for 15 min; control cells (A, τ_{Diff1} = 1.15 ms (36%), τ_{Diff2} = 8.14 ms (20%)) and cells preincubated for 3 days with 1 μM DMI (B, τ_{Diff1} = 0.59 ms (28%), τ_{Diff2} = 11.40 ms (4%)), hyperforin (C, τ_{Diff1} = 0.83 ms (24%), τ_{Diff2} = 12.00 ms (7%)), and hyperoside (D, τ_{Diff1} = 0.67 ms (16%), τ_{Diff2} = 11.32 ms (5%)).

(±0.36) ms (D_1 = 15.4 (±8.5) μm^2/s) and τ_{Diff2} = 9.37 (±3.38) ms (D_2 = 1.1 (±0.4) μm^2/s) (Figure 3A). Trajectories of single receptor−ligand complexes characterizing the lateral mobility of β_2-adrenergic receptors on the biomembrane of C6 cells after Alexa532-NA binding were measured by single particle tracking (SPT). An exemplary trajectory and the brightness of the probe as a function of time was plotted in Figure 4A,B. C6 cells stimulated with terbutaline showed increased diffusion time constants for the lateral mobility with τ_{Diff1} = 1.53 (±1.64) ms and τ_{Diff2} = 89.37 (±107.16) ms. Dissociation constants of K_{D1} = 3.97 (±1.26) nM and K_{D2} = 0.63 (±0.66) nM for the different mobility fractions could be derived from FCS saturation binding experiments with B_{max1} = 3.88 (±0.28) nM and B_{max2} = 0.98 (±0.14) nM representing low and high affinity states of the receptor−ligand complex (n = 36) (Figure 5). Treatment of cells with 1 μM of DMI, hyperforin, and

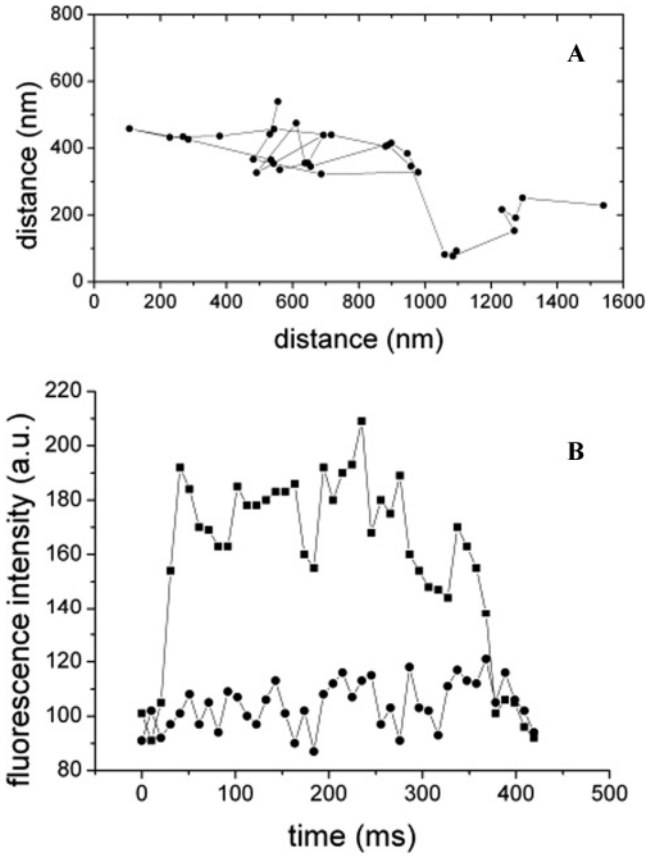

FIGURE 4: Trajectory (A) and fluorescence intensity (B, receptor−ligand complex (■), background fluorescence (●)) of a single β_2-adrenergic receptor after Alexa532-NA binding at C6 cells. Number of frames = 34, trajectory duration = 347 ms, D = 0.9 $\mu m^2/s$ calculated by mean square displacement analysis.

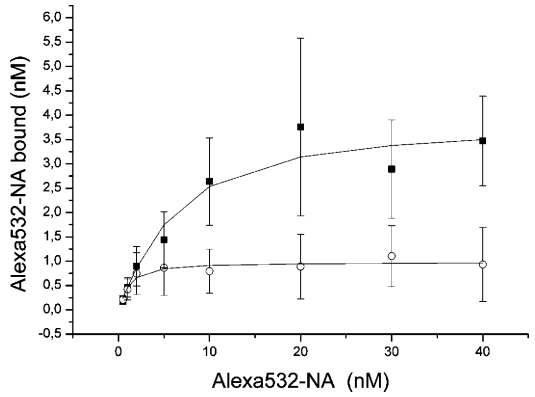

FIGURE 5: FCS saturation binding experiment with Alexa532-NA in the upper biomembrane of C6 cells. (■) Fraction of receptor−ligand complexes with τ_{Diff1}, (○) fraction of receptor−ligand complexes with τ_{Diff2}.

hyperoside, respectively, for 3 days decreased the Alexa532-NA binding significantly, compared to control cells (Figure 3B−D, Table 1). For treated cells similar diffusion time constants and diffusion coefficients, respectively, were found for the two different receptor−ligand states (Table 1). In untreated control cells the Alexa532-NA binding was distributed between the τ_{Diff1} and τ_{Diff2} fractions with a ratio of 1.9. Due to the fact that the reduction of β_2-AR binding in treated cells mainly correlated with a decrease in the τ_{Diff2} fraction, $\tau_{Diff1}/\tau_{Diff2}$ ratios increased to 5.3 for DMI, 3.4 for hyperforin, and 4.0 for hyperoside (Table 1). Decreased β_2-AR binding resulted in reduced intracellular cAMP formation in C6 cells when pretreated for 3 days with 1 μM of DMI, hyperforin, and hyperoside, respectively. Control cells revealed an increased chemiluminescence signal of 107 RLU (relative light units) for 6.33 pmol cAMP/25 000 cells after stimulation with 10 μM of terbutaline for 30 min compared to the basal values. Under the same conditions, pretreated cells showed a significant decrease in chemiluminescence of 47.4 (±26.3)% for DMI, 61.1 (±10.8)% for hyperforin, and 61.9 (±28.8)% for hyperoside (Figure 6) compared to control cells. For internalization studies HEK293 cells stably expressing a β_2-AR-GFP fusion protein (HEK293β2AR-GFP) were treated up to 6 days with 1 μM of DMI, hyperforin, and hyperoside, respectively. In contrast to control cells stimulated with 10 μM isoproterenol for 30 min (Figure 7B) exclusive treatment with DMI, hyperforin, and hyperoside, respectively, led to no internalization of β_2AR-GFP in these cells (Figure 7C,D,E).

DISCUSSION

Antidepressants mainly interfere with central neurotransmitter signaling, e.g., inhibition of either neurotransmitter reuptake or monoamine oxidase activity, followed by adaptive changes in the density of serotonin and β-adrenergic receptor (β-AR) subtypes. Synthetic selective serotonin-reuptake inhibitors (SSRI), serotonin-noradrenaline-reuptake inhibitors (SNRI), and tricyclic antidepressants (TCA), as well as St. John's Wort dry extracts are used for the treatment of depressive disorders. To further investigate the influence of hyperforin and hyperoside, major components of St. John's Wort dry extracts, on membrane associated receptors, we determined the binding behavior and lateral mobility of ligand activated β_2-adrenergic receptors (β_2-AR) after subchronic treatment of rat C6 glioblastoma cells, in comparison to desipramine (DMI).

C6 cells serve as an approved model for the investigation of regulatory processes at the single cellular level without any presynaptic input from neurotransmitters (*13*, *25*, *26*). Binding studies for the β_2-AR were performed using fluorescence correlation spectroscopy (FCS) and a fluorescently labeled noradrenaline derivative (Alexa532-NA) in C6 cells expressing the β_2-AR at low density on the cell surface (*27*, *28*). The β_2-selective binding behavior of Alexa532-NA has been described previously (*15*). A dose-dependent increase of intracellular cAMP level was found after incubation of C6 cells with Alexa532-NA and β_2-AR binding which clearly indicated the functionality of the ligand (Figure 1). Incubation of C6 cells with 10 nM Alexa532-NA resulted in a total binding of 4.26 (±0.53) nM. Two different diffusion time constants for the receptor−ligand complex were obtained with a fraction ratio $\tau_{Diff\ 1}/\tau_{Diff\ 2}$ of 1.9 (Figure 3A, Table 1). From the diffusion time constants $\tau_{Diff\ 1}$ and $\tau_{Diff\ 2}$, diffusion coefficients of D_1 = 15.4 (±8.5) $\mu m^2/s$ and D_2 = 1.1 (±0.4) $\mu m^2/s$ were calculated. Photobleaching of bound Alexa532-NA was investigated by measuring trajectories of single β_2-AR-Alexa532-NA complexes on the biomembrane of C6 cells. A typical trajectory of 34 frames over 347 ms and a spatial extent of approximately 0.5 × 1.6 μm^2 is given in Figure 4A. The evaluation of the brightness of each spot clearly demonstrated the photostability of Alexa532-NA, although minor blinking effects were found in the fluorescence intensity (Figure 4B). Thus, the different diffusion time constants for bound

Table 1: Binding Parameters of Alexa532-NA and Kinetics of Receptor−ligand Complexes (RLC) in C6 Cells[c]

	RLC							
	τ_{Diff1} [ms]	D_1 [μm^2/s]	τ_{Diff2} [ms]	D_2 [μm^2/s]	Alexa532-NA total binding [%]	fraction τ_{Diff1}, normalized	fraction τ_{Diff2}, normal ized	fraction ratio $\tau_{Diff1}/\tau_{Diff2}$
control	0.65 (± 0.36)	15.4 (± 8.5)	9.37 (± 3.38)	1.1 (± 0.4)	100 (± 12.4)	0.65 (± 0.12)	0.35 (± 0.10)	1.9
DMI[a]	0.61 (± 0.05)	16.4 (± 2.7)	14.31 (± 10.76)	0.7 (± 0.5)	62.0 (± 12.6)*[b]	0.84 (± 0.20)	0.16 (± 0.08)	5.3
hyperforin[a]	0.87 (± 0.26)	11.5 (± 4.0)	9.58 (± 3.66)	1.0 (± 0.4)	53.1 (± 9.3)***[b]	0.77 (± 0.12)	0.23 (± 0.12)	3.4
hyperoside[a]	0.80 (± 0.27)	12.5 (± 4.2)	10.70 (± 5.29)	0.9 (± 0.5)	59.4 (± 8.8)**[b]	0.80 (± 0.14)	0.20 (± 0.03)	4.0

[a] C6 cells preincubated with 1 μM desipramine (DMI), 1 μM hyperforin, 1 μM hyperoside for 3 days, respectively. [b] $p^* < 0.05$; $p^{**} < 0.01$; $p^{***} < 0.001$. [c] $n = 72$.

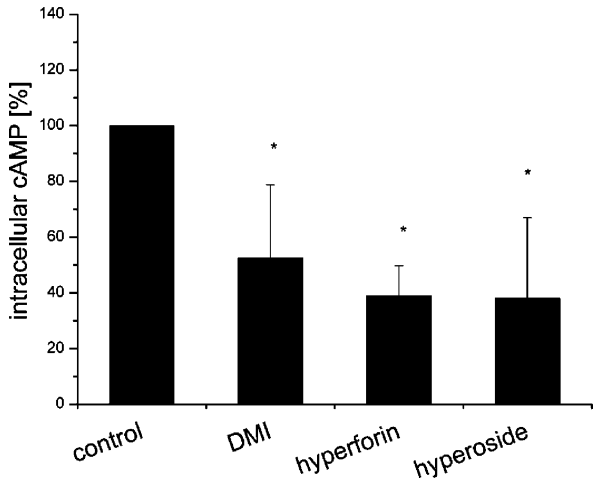

FIGURE 6: Accumulation of intracellular cAMP in C6 cells after stimulation with 10 μM terbutaline for 30 min. Control cells and cells preincubated for 3 days with 1 μM DMI, hyperforin, and hyperoside. Differences between basal cAMP levels and terbutaline-stimulated cAMP are presented ($n = 3$) (*$p < 0.05$).

Alexa532-NA molecules were not caused by photobleaching effects. Slower diffusion time constants for β_2-AR ligand complexes in hippocampal neurons and alveolar type II cells (A549) with $\tau_{Diff\ 1} = 1.8$ and 3.3 ms, and $\tau_{Diff\ 2} = 158.6$ and 95.2 ms, respectively, have been published recently (*15*). In these cells the fraction of hindered, i.e., slower lateral receptor mobility was clearly increased during internalization processes. Similar results were found for the $GABA_A$ and the benzodiazepine receptor (*16*, *21*). Thus, differences in τ_{Diff2} may result from the different cell types and their different internalization behavior after β_2-AR stimulation with Alexa532-NA in nanomolar concentrations. Comparison of β_2-AR down-regulation to internalization in BEAS-2B cells showed that weak agonist stimulation caused down-regulation in the absence of significant internalization (*28*). To detect internalized receptor−ligand complexes, C6 cells stimulated with 10 nM Alexa532-NA were scanned by moving a sharply focused laser beam along the *z*-direction. Individual fluorescent events correlating with the appearance of receptor−ligand complexes in the cytoplasm were not found in contrast to C6 cells which were stimulated with 10 nM Alexa532-NA together with 1 μM of terbutaline (Figure 2). Under the same conditions *z*-scans with intensive events in the fluorescence track indicating internalized β_2-AR have been published for A549 cells (*15*). From saturation binding experiments low and high affinity states of receptor−ligand complexes were found with dissociation constants of $K_{D1} = 3.97$ (±1.26) nM and $K_{D2} = 0.63$ (±0.66) nM which correlated with the mobility fractions $\tau_{Diff\ 1}$ and $\tau_{Diff\ 2}$, respectively. Preincubation of C6 cells with DMI led to a reduction in total Alexa532-NA binding of 38.0% mainly caused by a decrease in the high-affinity receptor−ligand fraction with $\tau_{Diff\ 2}$ (Table 1, Figure 3B). Whereas values for $\tau_{Diff\ 1}$ and $\tau_{Diff\ 2}$ stayed almost unchanged, the fraction ratio $\tau_{Diff\ 1}/\tau_{Diff\ 2}$ changed significantly from 1.9 to 5.3 (Table 1). A decrease in total β-AR density after DMI treatment has also been shown in C6 cells in radioreceptor assay experiments (*27*). Interestingly, HEK293 cells overexpressing β_2-AR as a GFP-fusion construct showed no receptor internalization after DMI treatment. Our findings lead us to the conclusion that reduction in total Alexa532-NA binding is due to a decrease in the formation of the receptor−ligand complex with $\tau_{Diff\ 2}$ in the high affinity state which was described before as the high conformational receptor state resulting from the temporary ligand−receptor−G_s-protein trimer (*30*). One possible explanation could be changes in the interaction of occupied receptors with regulatory proteins like G_s-protein after DMI treatment, already reported for neutrophile β_2-AR after treatment of panic disorder (PD) patients with the structurally related imipramine (*31*). Alterations in the interaction of G_s-protein and β-AR, with resulting changes in the ratio of high and low conformational receptor states, have also been demonstrated after preincubation of C6 cells with DMI (*12*, *13*, *32*). In our experiments similar results have been obtained with C6 cells preincubated with hyperforin and hyperoside, respectively. A decrease in total Alexa-NA binding of 46.9% for hyperforin and 40.6% for hyperoside was observed, characterized by a shift of the corresponding autocorrelation curves on the FCS time scale (Table 1, Figure 3C,D). Despite GFP-tagged β_2-AR's showing no internalization in the presence of hyperforin and hyperoside in our experiments, a decrease in β-AR density in rats after treatment for 2 weeks with a hyperforin-rich St. John's Wort extract has been reported, although this study did not differentiate between receptor subtypes (*7*). DMI-like results were found for the fraction ratio $\tau_{Diff\ 1}/\tau_{Diff\ 2}$, which was 3.4 for hyperforin and 4.0 for hyperoside, caused by a significant decrease in the number of high affinity β_2-AR-ligand complexes with $\tau_{Diff\ 2}$. The resulting reduction in β_2-adrenergic sensitivity of C6 cells under the influence of DMI, hyperforin, and hyperoside, respectively, was demonstrated by a reduction of intracellular cAMP concentration after stimulation with terbutaline (Figure 6). For DMI such an influence on β-AR and downstream cAMP production in C6 cells has already been reported using radioreceptor assay (*12*, *13*, *27*). For hyperforin and hyperoside, however, a reduced responsiveness of the β_2-adrenergic stimulated AC/cAMP signaling pathway is, to our knowledge, reported here for the first time. Antidepressant effects of hyperforin and hyperoside from St.

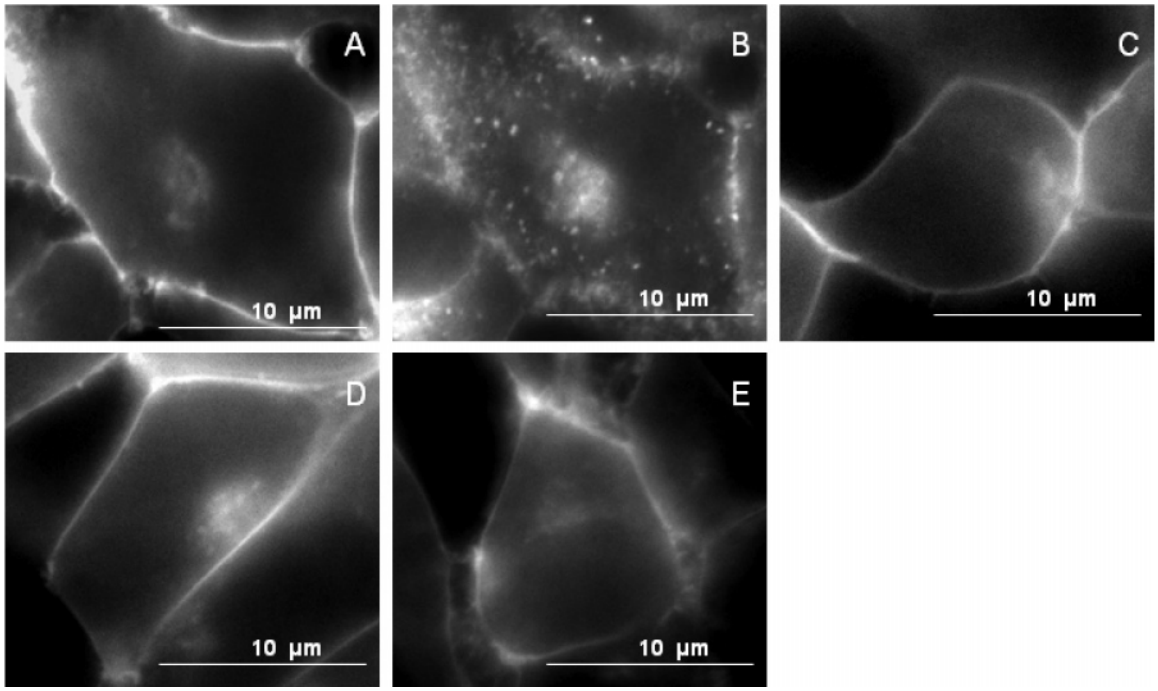

FIGURE 7: Fluorescence microscopy of HEK293β_2AR-GFP cells. (A) Unstimulated control cells; (B) control cells stimulated with 10 μM isoprenaline for 20 min; (C) cells incubated with 1 μM DMI for 6 days; (D) cells incubated with 1 μM hyperforin for 6 days; (E) cells incubated with 1 μM hyperoside for 6 days.

John's Wort in in vitro and animal models have been described previously (*7*, *9*, *10*, *33*). The mode of action of synthetic antidepressants, as well as of St. John's Wort, is basically attributed to synaptic communication of the neurotransmitters noradrenaline and serotonin. Effects of single compounds from St. John's Wort on the postsynaptic regulation of β_2-AR have not yet been described. A more detailed view on such effects concerning receptor subtypes is of interest because it has been shown that the ratio of the β_1-/β_2-AR distribution in cells influences AC activity differently (*34*, *35*). Our work presents data on the reduction in β_2-adrenergic sensitivity of C6 cells with the isolated compounds hyperforin and hyperoside. It therefore provides an insight into the mode of action and the therapeutic relevance of St. John's Wort preparations for the treatment of mild to moderate depression and anxiety symptoms.

ACKNOWLEDGMENT

Rat C6 glioblastoma cells were a kind gift from Th. Franz, Department of Anatomy, Rheinische Friedrich-Wilhelms University of Bonn. The plasmid encoding for the β_2-AR-GFP fusion protein was a kind donation of M. J. Lohse, Department of Pharmacology and Toxicology, University of Würzburg. We thank U. Kubitscheck, Institute of Physical and Theoretical Chemistry, Rheinische Friedrich-Wilhelms University of Bonn, for support and comments on single particle tracking and track analysis.

REFERENCES

1. Taylor, C., Fricker, A. D., Devi, L. A., and Gomes, I. (2005) Mechanisms of action of antidepressants: from neurotransmitter systems to signaling pathways, *Cell. Signalling 17* (5), 549−557.
2. Ackenheil, M. (1990) The mechanism of action of antidepressants revised, *J. Neural Transm. Suppl. 32*, 29−37.
3. Bourin, M., and Baker, G. B. (1996) The future of antidepressants, *Biomed. Pharmacother. 50* (1), 7−12.
4. Greeson, J. M., Sanford, B., and Monti, D. A. (2001) St. John's wort (Hypericum perforatum): a review of the current pharmacological, toxicological, and clinical literature, *Psychopharmacology 153* (4), 402−414.
5. Vetulani, J., and Sulser, F. (1975) Action of various antidepressant treatments reduces reactivity of noradrenergic cyclic AMP-generating system in limbic forebrain, *Nature 257* (5526), 495−496.
6. Racagni, G., and Brunello, N. (1984) Transynaptic mechanisms in the action of antidepressant drugs, *Trends Pharmacol. Sci. 5*, 527−531.
7. Müller, W. E., Singer, A., Wonnemann, M., Hafner, U., Rolli, M., and Schafer, C. (1998) Hyperforin represents the neurotransmitter reuptake inhibiting constituent of hypericum extract, *Pharmacopsychiatry 31* (Suppl. 1), 16−21.
8. Singer, A., Wonnemann, M., and Müller, W. E. (1999) Hyperforin, a major antidepressant constituent of St. John's Wort, inhibits serotonin uptake by elevating free intracellular Na+1, *J. Pharmacol. Exp. Ther. 290* (3), 1363−1368.
9. Butterweck, V., Jurgenliemk, G., Nahrstedt, A., and Winterhoff, H. (2000) Flavonoids from Hypericum perforatum show antidepressant activity in the forced swimming test, *Planta Med. 66* (1), 3−6.
10. Butterweck, V., Hegger, M., and Winterhoff, H. (2004) Flavonoids of St. John's Wort reduce HPA axis function in the rat, *Planta Med. 70* (10), 1008−1011.
11. Chen, J., and Rasenick, M. M. (1995) Chronic treatment of C6 glioma cells with antidepressant drugs increases functional coupling between a G protein (Gs) and adenylyl cyclase, *J. Neurochem. 64* (2), 724−732.
12. Manji, H. K., Chen, G. A., Bitran, J. A., Gusovsky, F., and Potter, W. Z. (1991) Chronic exposure of C6 glioma cells to desipramine desensitizes beta-adrenoceptors, but increases KL/KH ratio, *Eur. J. Pharmacol. 206* (2), 159−162.
13. Manji, H. K., Chen, G. A., Bitran, J. A., and Potter, W. Z. (1991) Down-regulation of beta receptors by desipramine in vitro involves PKC/phospholipase A2, *Psychopharmacol. Bull. 27* (3), 247−253.
14. Bürgi, S., Baltensperger, K., and Honegger, U. E. (2003) Antidepressant-induced switch of beta 1-adrenoceptor trafficking as a mechanism for drug action, *J. Biol. Chem. 278* (2), 1044−1052.
15. Hegener, O., Prenner, L., Runkel, F., Baader, S. L., Kappler, J., and Haberlein, H. (2004) Dynamics of beta2-adrenergic receptor-ligand complexes on living cells, *Biochemistry 43* (20), 6190−6199.

16. Meissner, O., and Häberlein, H. (2003) Lateral mobility and specific binding to GABA(A) receptors on hippocampal neurons monitored by fluorescence correlation spectroscopy, *Biochemistry 42* (6), 1667−1672.
17. Brock, R., Vamosi, G., Vereb, G., and Jovin, T. M. (1999) Rapid characterization of green fluorescent protein fusion proteins on the molecular and cellular level by fluorescence correlation microscopy, *Proc. Natl. Acad. Sci. U.S.A. 96* (18), 10123−10128.
18. Bacia, K., Kim, S. A., and Schwille, P. (2006) Fluorescence cross-correlation spectroscopy in living cells, *Nat. Methods 3* (2), 83−89.
19. Middleton, R. J., and Kellam, B. (2005) Fluorophore-tagged GPCR ligands, *Curr. Opin. Chem. Biol. 9* (5), 517−525.
20. Briddon, S. J., Middleton, R. J., Cordeaux, Y., Flavin, F. M., Weinstein, J. A., George, M. W., Kellam, B., and Hill, S. J. (2004) Quantitative analysis of the formation and diffusion of A1-adenosine receptor-antagonist complexes in single living cells, *Proc. Natl. Acad. Sci. U.S.A. 101* (13), 4673−4678.
21. Hegener, O., Jordan, R., and Häberlein, H. (2002) Benzodiazepine binding studies on living cells: application of small ligands for fluorescence correlation spectroscopy, *Biol. Chem. 383* (11), 1801−1807.
22. Widengren, J., and Schwille, P. (2000) Characterization of photoinduced isomerization and back-isomerization of the cyanine dye Cy5 by fluorescence correlation spectroscopy, *J. Phys. Chem. A 104* (27), 6416−6428.
23. Marquardt, D. W. (1963) An algorithm for least-squares estimation of nonlinear parameters, *J. Soc. Indust. Appl. Math. 11*, 431−441.
24. Krasel, C., Bunemann, M., Lorenz, K., and Lohse, M. J. (2005) Beta-arrestin binding to the beta2-adrenergic receptor requires both receptor phosphorylation and receptor activation, *J. Biol. Chem. 280* (10), 9528−9535.
25. Fishman, P. H., Miller, T., Curran, P. K., and Feussner, G. K. (1994) Independent and coordinate regulation of beta 1- and beta 2-adrenergic receptors in rat C6 glioma cells, *J. Recept. Res. 14* (5), 281−296.
26. Kientsch, U., Bürgi, S., Ruedeberg, C., Probst, S., and Honegger, U. E. (2001) St. John's wort extract Ze 117 (Hypericum perforatum) inhibits norepinephrine and serotonin uptake into rat brain slices and reduces 3-adrenoceptor numbers on cultured rat brain cells, *Pharmacopsychiatry 34* (Suppl. 1), 56−60.
27. Fishman, P. H., and Finberg, J. P. (1987) Effect of the tricyclic antidepressant desipramine on beta-adrenergic receptors in cultured rat glioma C6 cells, *J. Neurochem. 49* (1), 282−289.
28. Kiely, J., Hadcock, J. R., Bahouth, S. W., and Malbon, C. C. (1994) Glucocorticoids down-regulate beta 1-adrenergic-receptor expression by suppressing transcription of the receptor gene, *Biochem. J. 302* (Part 2), 397−403.
29. Williams, B. R., Barber, R., and Clark, R. B. (2000) Kinetic analysis of agonist-induced down-regulation of the β_2-adrenergic receptor in BEAS-2B cells reveals high- and low-affinity components, *Mol. Pharmacol. 58* (2), 421−430.
30. Gilman, A. G. (1989) The Albert Lasker Medical Awards. G proteins and regulation of adenylyl cyclase, *JAMA, J. Am. Med. Assoc. 262* (13), 1819−1825.
31. Gurguis, G. N., Blakeley, J. E., Antai-Otong, D., Vo, S. P., Orsulak, P. J., Petty, F., and Rush, A. J. (1999) Adrenergic receptor function in panic disorder. II. Neutrophil beta 2 receptors: Gs protein coupling, effects of imipramine treatment and relationship to treatment outcome, *J. Psychiatr. Res. 33* (4), 309−322.
32. Manier, D. H., Bieck, P. R., Duhl, D. M., Gillespie, D. D., and Sulser, F. (1992) The beta-adrenoceptor-coupled adenylate cyclase system in rat C6 glioma cells. Deamplification by isoproterenol and oxaprotiline, *Neuropsychopharmacology 7* (2), 105−112.
33. Chatterjee, S. S., Bhattacharya, S. K., Wonnemann, M., Singer, A., and Müller, W. E. (1998) Hyperforin as a possible antidepressant component of hypericum extracts, *Life Sci. 63* (6), 499−510.
34. Zhong, H., Guerrero, S. W., Esbenshade, T. A., and Minneman, K. P. (1996) Inducible expression of beta 1- and beta 2-adrenergic receptors in rat C6 glioma cells: functional interactions between closely related subtypes, *Mol. Pharmacol. 50* (1), 175−184.
35. Guerrero, S. W., Zhong, H., and Minneman, K. P. (1995) Selective desensitization of beta 1- and beta 2-andrenergic receptors in C6 glioma cells. Effects on catecholamine responsiveness, *Receptor 5* (4), 185−195.

BI6025819